Manganese-induced hyperactivity and dopaminergic dysfunction depend on age, sex and YAC128 genotype

Jordyn M. Wilcox[1,2,#], David C. Consoli[1,2], Krista C. Paffenroth[2], Brittany D. Spitznagel[1,2], Erin S. Calipari[2,3], Aaron B. Bowman[4], Fiona E. Harrison[1,2]

[1]Division of Diabetes, Endocrinology and Metabolism, Department of Medicine, Vanderbilt University Medical Center, Nashville, TN

[2]Vanderbilt Brain Institute, Vanderbilt University, Nashville, TN

[3]Departments of Pharmacology, Molecular Physiology and Biophysics, Psychiatry and Behavioral Sciences; Vanderbilt Center for Addiction Research, Vanderbilt University, Nashville, TN

[4]School of Health Sciences, Purdue University, West Lafayette, IN

Abstract

Manganese (Mn) is an essential micronutrient but is neurotoxic in excess. Environmental and genetic factors influence vulnerability to Mn toxicity, including sex, age, and the autosomal dominant mutation that causes Huntington disease (HD). To better understand the differential effects of Mn in wild-type (WT) versus YAC128 mice, we examined impacts of Mn exposure across different ages and sexes on disease-relevant behavioral tasks and dopamine dynamics. Young (3-week) and aged (12-month) WT and YAC128 mice received control (70 ppm) or high (2400 ppm) Mn diet for 8 weeks followed by a battery of behavioral tasks. In young female WT mice, high Mn diet induced hyperactivity across two independent behavioral tasks. Changes in the expression of tyrosine hydroxylase (TH) were consistent with the behavioral data in young females such that elevated TH in YAC128 on control diet was decreased by high Mn diet. Aged YAC128 mice showed the expected disease-relevant behavioral impairments in females and decreased TH expression, but we observed no significant effects of Mn diet in either genotype of the aged group. Fast-scan cyclic voltammetry recorded dopamine release and clearance in the nucleus accumbens of eight-month-old WT and YAC128 mice following acute Mn exposure (3x/1 week subcutaneous injections of 50 mg/kg MnCl[2]-tetrahydrate or saline). In WT mice,

#corresponding author: Jordyn M. Wilcox, PhD, jordyn.wilcox@vumc.org, 2215 Garland Ave, Medical Research Building IV, 7445, Nashville, TN 37232.

Conflict of Interest Statement: The authors declare no conflicts of interest.

Mn exposure led to faster dopamine clearance that resembled saline treated YAC128 mice. Mn treatment increased dopamine release only in YAC128 mice, possibly indirectly correcting the faster dopamine clearance observed in saline treated YAC128 mice. The same exposure paradigm led to decreased dopamine and serotonin and metabolites (3-MT, HVA and 5-HIAA) in striatum and increased glutamate in YAC128 mice but not WT mice. These studies confirm an adverse effect of Mn in young, female WT animals and support a role for Mn exposure in stabilizing dopaminergic dysfunction and motivated behavior in early HD.

Keywords

manganese; dopamine; behavior; Huntington; YAC128

1. Introduction

Sufficient manganese (Mn) for optimal health is acquired via the diet (Horning, Caito, Tipps, Bowman, & Aschner, 2015; Martins et al., 2020), however, Mn homeostasis is influenced by exposure route, sex, age, and disease state (Erikson, Thompson, Aschner, & Aschner, 2007; Madison, Wegrzynowicz, Aschner, & Bowman, 2011; Taylor et al., 2019; Winslow, Limesand, & Zhao, 2020). Mn is an essential micronutrient but overexposure can lead to neurotoxicity. While toxic effects are more commonly observed following inhalation exposures, toxic oral exposures can occur despite tight regulation of Mn absorption at the level of the gastrointestinal tract (Chen, Bornhorst, & Aschner, 2018). Oral consumption of excessive Mn occurs from drinking contaminated water sources including well water (Frisbie, Ortega, Maynard, & Sarkar, 2002), and in the case of infants, drinking soy-based formula (Frisbie et al., 2019). A growing body of research has implicated high Mn exposure in early life in the development of attention-deficit/hyperactivity disorder (ADHD) (Schullehner et al., 2020) and deficits in neurocognitive function (C. H. Kern, Stanwood, & Smith, 2010; C. Kern, Stanwood, & Smith, 2011; Tran et al., 2002), suggesting toxic early exposures contribute to disease pathology.

Several neuronal and glial processes are disrupted following excess manganese (Mn) exposure, but the specific underlying mechanisms are not well understood. Increased production of reactive oxygen and nitrogen species, mitochondrial dysfunction and apoptosis are all strongly implicated in Mn toxicity (Fernandes et al., 2017; Kitazawa, Wagner, Kirby, Anantharam, & Kanthasamy, 2002; Martinez-Finley, Gavin, Aschner, & Gunter, 2013; M. D. Neely, Davison, Aschner, & Bowman, 2017; Warren et al., 2020; Yang et al., 2019). Neuroinflammation including microglial release of proinflammatory cytokines is also hypothesized to play a role in Mn toxicity (Kirkley, Popichak, Afzali, Legare, & Tjalkens, 2017; Wang et al., 2017). Prior to cell death, Mn directly impacts neurological function by altering several neurotransmitter systems (Balachandran et al., 2020). Excess Mn exposure during the early postnatal period in rats altered signaling of several biogenic amines in adulthood (dopamine (DA), norepinephrine (NE), serotonin (5-HT) (Lasley et al., 2020)). The glutamatergic, GABAergic and dopaminergic systems have been at the forefront of Mn neurotoxicity research given the selective accumulation of Mn in basal ganglia

structures and the movement disorders that occur following excess exposure (Fitsanakis, Au, Erikson, & Aschner, 2006; Robison, Sullivan, Cannon, & Pushkar, 2015).

Both dopaminergic and glutamatergic signaling are disrupted in the inherited progressive neurodegenerative disorder Huntington's Disease (HD) (André, Cepeda, & Levine, 2010; Joshi et al., 2009). Animal and cell models of HD are resistant to Mn toxicity and display blunted responses to both acute and chronic systemic injection Mn exposures (Pfalzer et al., 2020; Wilcox et al., 2021; Williams, Li, et al., 2010). In the present study, we explored the HD-Mn interaction in response to excess dietary Mn. We hypothesized that high Mn dietary intervention would yield neurotoxic damage resulting in altered dopaminergic function and related behavioral changes in young and aged wild-type (WT) mice, and that YAC128 mice would be protected from these toxic effects at both ages. Further, we hypothesized that females would be more greatly affected based on differences in Mn metabolism and case reports of Mn toxicity (Broberg et al., 2019; Gibson, Anderson, & Sabry, 1983; Schuh, 2016; Schullehner et al., 2020). We sought to further examine the HD-Mn interaction by probing *ex vivo* dopaminergic dynamics and striatal tissue neurotransmitter metabolism following acute (1-week) *in vivo* Mn exposure at a middle-age, at the cusp of significant neuronal loss observed in YAC128 mice (Slow et al., 2003). The treatment schedules were designed to assess whether YAC128 were merely resistant to Mn-induced damage compared to WT mice, or whether Mn may in fact have therapeutic potential against HD-like phenotypes in the transgenic animals.

2. Methods

2.1 Animals

Animal husbandry and genotyping has been previously described (Pfalzer et al., 2020). The current study used YAC128 mice backcrossed onto the C57BL/6J background (YAC128-C57) and their wild-type (WT) littermates. HD phenotypes are penetrant on the C57BL/6J background but are not as severe as observed in the original YAC128 FVB/NJ strain (Van Raamsdonk et al., 2007). Mice were weaned at 21 days and housed in groups of 3-5 of a single sex in a temperature- and humidity-controlled housing room on a 12:12 light:dark cycle with food and water available *ad libitum.* Approximately equal numbers of male and female mice were used in each genotype-diet and genotype-treatment group. All protocols were approved by the Vanderbilt University Institutional Animal Care and Use Committee under protocol numbers M1600073 and M1900090. All experiments were conducted in accordance with the NIH Guide for the Care and Use of Laboratory Animals. Three distinct cohorts of mice were used in the following studies: 1) young dietary Mn intervention, 2) aged dietary Mn intervention, 3) middle-aged acute Mn injection (separate mice for FSCV and neurotransmitter measurements).

2.2 Dietary Mn intervention

Standard lab chow (LabDiet 5L0D, TX) containing approximately 70 ppm Mn (variable based on batch) was available *ad libitum* prior to dietary intervention. For dietary intervention mice were put on specially formulated diets (Research Diets, Inc.) that contained 70 ppm (control) or 2400 ppm Mn (high). Other micro- and macronutrient content

was consistent between the two diets. The high Mn diet was chosen based previous reports that this Mn content significantly increased brain Mn after 30 days (Jenkitkasemwong et al., 2018). Diet was randomly assigned to a cage prior to behavioral testing.

Mice in the young experimental group were put on experimental diet at weaning (3 weeks of age; prior to genotyping) and were tested on a battery of behavioral tests at 11 weeks of age prior to sacrifice and dissection at 12 weeks of age (Fig. 1A). Mice in the aged experimental group were weaned at 3 weeks of age and were maintained on regular chow until a pre-intervention behavioral battery at approximately 11.5 months of age. Aged mice were then placed on experimental diet at 12 months of age, and 8 weeks later at approximately 14 months of age underwent a post-diet behavioral battery prior to sacrifice and dissection at approximately months of age (Fig. 2A).

2.3   Acute manganese injections

Manganese chloride tetrahydrate ($MnCl_2 \cdot 4(H_2O)$, Fisher Scientific) was made up in deionized water as a 1% stock solution, filtered through a 0.2 μm membrane, and administered as 50 mg/kg body weight. Saline (0.9%) was used as a control injection. Treatment was administered at a volume of 5 mL/kg injected subcutaneously in the left or right (alternating) inguinal area using an insulin syringe (27 G, ½ inch). The 50 mg/kg $MnCl_2 \cdot 4(H_2O)$ dose corresponds to a dose of 13.8 mg/kg Mn^{2+}. Mice were exposed acutely (1-week exposure) at 8-9 months of age using a previously adapted exposure paradigm (Dodd, Ward, & Klein, 2005) known to significantly increase brain Mn (Pfalzer et al., 2020). Mice were injected on days 1, 4, and 7 prior to sacrifice and fast scan cyclic voltammetry (*see* Fig. 5) or dissection on day 8 (24 hours after the final injection, *see* Fig. 6).

2.5   Behavioral testing

2.5.1   Experimental groups.—Young mice: WT control diet = 6F, 8M; WT high Mn diet = 7F, 5M; YAC128 control diet=7F, 8M; YAC128 high Mn diet= 5F, 11M. Aged mice: WT control diet = 7F, 7M; WT high Mn diet = 8F, 7M; YAC128 control diet=9F, 3M; YAC128 high Mn diet= 8F, 3M. Compared to females, fewer aged YAC128 male mice were included due to aggression and separation from cagemates.

2.5.2   Test order.—For young mice: Day 1: Elevated Zero Maze (EZM), Day 2: Locomotor activity, grip strength, Days 3-5: Rotarod. For aged mice, the same behavioral battery was performed pre- and post-diet intervention: Day 1: EZM, Day 2: Locomotor activity, grip strength, Days 3-5: Rotarod, Day 8: Y-maze alternation, Day 10: Nest building and food consumption.

2.5.3   Elevated zero maze (EZM).—A standard white elevated zero maze (EZM; San Diego Instruments, CA) was used to assess anxiety-like and exploratory behavior. Time spent in the open zone (s) and total distance travelled over 5 minutes was recorded by a camera suspended from the ceiling and analyzed using AnyMaze (Stoelting Co., IL).

2.5.4   Locomotor activity.—Spontaneous locomotor activity was measured by breaking of infrared beams over 30 minutes in standard sound-attenuating, light- and air-controlled locomotor activity chambers (27 x 27 x 20.5 cm, ENV-510; MED Associates, VT).

2.5.5   Grip strength.—Grip strength was measured using a force meter (San Diego Instruments, San Diego, CA). Mice were allowed to firmly grip a square wire grid with the two front paws while being held by the tail. The experimenter gently pulled the mouse back the in a horizontal plane until the grip was broken, and maximum force (N) was measured automatically by the apparatus. Each mouse was given three trials and average force per mouse was used for analysis. The same experimenter performed grip strength for all mice to decrease inter-experimenter variability.

2.5.6   Rotarod.—Rotarod performance was assessed as a proxy for motor coordination and motor learning using a standard rotarod apparatus (Ugo Basile). The rod was 3 cm in diameter, suspended approximately 25 cm above a plastic lever on to which mice fell. There were five equal compartments (6 cm length of rod) divided by beige plexiglass. A different accelerating protocol was used for young and aged mice. For young, the rod began rotating at 4 rpm and ramped up to a max speed of 40 rpm by 4 min (total test time 5 min, max speed for final min). Ramp speed increased to max speed over 5 minutes for aged mice. The rod was rotating at 4 rpm when mice were placed on the apparatus and a timer was started, recording the latency to fall from the rod. Mice completed three trials per day, max 5 min per trial, with inter-trial intervals of 15 - 30 min. The daily average time to fall for each mouse was used in analysis of data.

2.5.7   Y-maze alternation.—A closed, rounded top Y-maze made of clear acrylic tubing with arms 32-cm long was used to assess short-term spatial memory. Spontaneous alternation was measured in a single 6-minute trial. Mice explored freely as an experimenter blind to genotype and diet scored arm entries from an adjacent room via live video recording taken overhead the maze. Arm entries were only counted if the entire body of the mouse (all four paws and half of tail) entered the arm. Alternation was defined as consecutive entry into three different arms (e.g., ABC but not ABA). Percent alternation was calculated as [alternations/(total arm entries-2)] x 100.

2.5.8   Nest building.—Mice were individually housed overnight (transferred from group housing just prior to start of dark cycle) in clean cages with standard bedding and two cotton nestlets (5 g; Ancare, NY). The following morning, un-shredded nestlet material was weighed and an experimenter blind to genotype and diet scored the nest quality on a scale between 0 – 5, adapted to include half-point increments where 5 represents a 3-dimensional nest incorporating almost all of the shredded bedding (Deacon, 2006).

2.5.9   Food consumption.—During the nest building task when mice were single housed, food was pre-weighed (approximately 5-10 g) prior to placing the mouse in the cage. The following morning, the remaining food was weighed to calculate food consumed overnight.

2.6   Biochemical experiments following dietary intervention

2.6.1   Tissue collection.—Approximately 48-72 hours following completion of the behavioral battery, mice were anesthetized using isoflurane prior to cervical dislocation and decapitation. The brain was removed, weighed, and striatum from both hemispheres collected by microdissection. Tissue was snap frozen on dry ice and stored at −80°C until used for biochemical analyses. Young mice: WT control diet = 8F, 8M; WT high Mn diet = 8F, 5M; YAC128 control diet=8F, 8M; YAC128 high Mn diet= 7F, 11M. Aged mice: WT control diet = 6F, 7M; WT high Mn diet = 7F, 7M; YAC128 control diet=8F, 3M; YAC128 high Mn diet= 8F, 3M. Compared to females, fewer aged YAC128 male mice were included due to aggression and separation from cagemates.

2.6.2   Mn levels.—Mn concentrations were measured by inductively coupled plasma mass spectrometry (ICP-MS) from a protein lysate (described below) using the methods previously described (Pfalzer et al., 2020). Briefly, 50 uL protein lysate was digested at a 1:1 dilution in ultrapure nitric acid (70%) for 48 hours at 50 °C (water bath); 100 uL of digested tissue was further diluted to 2% nitric acid with DI water and Mn analyzed.

2.6.3   Western blotting.—Protein lysates were prepared by homogenizing frozen tissue by hand with a plastic pestle in 200 uL Pierce RIPA lysis buffer (Thermo Scientific, cat # 89900) with protein and phosphatase inhibitors [cOmplete™ EDTA-free protease inhibitor cocktail (Roche, 04693132001), 1:100 phosphatase inhibitor cocktail 3 (MilliporeSigma, cat.no. P0044), and 1 mM sodium orthovanadate per 10 ml of RIPA buffer (Thermo Fisher Scientific, cat # 89900)]. Protein lysate was collected following centrifugation at 12,000 g for 5 min. Protein concentration was measured using standard bicinchoninic acid (BCA) assay protocol (Pierce BCA Protein Assay Kit, Thermo Scientific). Samples were denatured with NuPage LDS sample buffer (Thermo Scientific, cat # NP0007) and reducing agent (Thermo Scientific, cat # NP0009) and boiled at 95 °C for 3 minutes prior to loading on Bolt™ 4-12% Bis-Tris Plus gels (Thermo Scientific, cat # NW04120BOX). Protein was transferred to nitrocellulose membranes using the iBlot2™ system (Thermo Scientific, cat # IB23001). Gels were rehydrated overnight in DI water and stained with Coomassie blue (Bio-Rad, cat # 161-0786) for total protein used as loading control. Three sets of gels were run because of overlapping molecular weights and protein loading requirements. For pTH Ser31 and TH (anti-rabbit, Cell Signaling Technologies, cat # 3370 and 2792) 20 ug protein was loaded per well. For pERK1/2 and ERK1/2 (P-p44/42 MAPK and p44/42 MAPK, anti-rabbit, Cell Signaling Technologies, cat # 4370 and 9102) 40 ug protein was loaded. For DAT (anti-rat, Millipore Sigma, cat # MAB369) and SLC30A10 (anti-rabbit, Abcam, cat # ab229954) 20 ug protein was loaded per well. Specificity and authenticity for each of the antibodies is documented by the respective vendor. Following transfer, membranes were blocked for 30 min with 5% nonfat milk in tris-buffered saline with 0.1% Tween-20 (TBST) and then 30 min in 5% bovine albumin serum (BSA) in TBST. Blots were incubated in primary antibody (1:1,000 in 5% BSA in TBST) overnight at 4 °C followed by appropriate secondary antibody incubation (1:5,000 in 5% nonfat milk) for 2 hours. Protein bands were visualized using chemiluminescence (Western Lighting Plus ECL, Perkin Elmer, cat # 103E001EA). Phosphoproteins were probed first, and membranes stripped (Restore Stripping Buffer, Thermo Fisher Scientific, cat # 21059) before probing the total protein

(TH and ERK1/2). For young mice, males and females were run on separate blots with 2-3 samples from each genotype-diet group per gel. Both sexes were run on the same gels for aged mice. Protein bands were quantified using ImageJ (imagej.nih.gov). Each protein band was normalized to its own total protein (Coomassie blue stained gel) as a loading control, and then to average WT control diet for that blot.

2.7 Fast-scan cyclic voltammetry (FSCV)

FSCV was performed as previously described (Consoli, Brady, Bowman, Calipari, & Harrison, 2020). Briefly, mice were sacrificed by decapitation without anesthesia. The whole brain was removed and placed into cold-oxygenated artificial cerebral spinal fluid (aCSF) with 126 mM NaCl, 2.5 mM KCl, 1.2 mM NaH_2PO_4, 2.4 mM $CaCl_2$, 1.2 mM $MgCl_2$, 25 mM $NaHCO_3$, 0.4 mM ascorbate, and 11 mM glucose with pH adjusted to 7.4. Using a vibratome, 300 μM thick coronal sections were taken and allowed to equilibrate for 30 min at room temperature (22 °C) in a holding chamber containing oxygenated aCSF. Sections were moved to a testing chamber containing aCSF with a flow rate of lml/min at 32 °C. Extracellular dopamine was measured in the core of the nucleus accumbens using a cylindrical carbon fiber microelectrode and a bipolar stimulating electrode (Fig. 5A). Voltammetry data were collected and modeled using Demon Voltammetry and Analysis Software (Yorgason, España, & Jones, 2011).

For peak and return to baseline measurements computations were based on user-defined positions on current traces. Tau values were determined from exponential fit curves based on the peak and the post-peak baseline using a least squares constrained exponential fit algorithm (National Instruments). Peak height (in nA) was determined by the peak of the evoked signal.

For FSCV experimental groups were as follows: WT veh = 3F, 2M; WT Mn = 3F, 2M; YAC128 veh =3F, 1M; YAC128 Mn = 2F, 2M.

2.8 Neurotransmitter and metabolite measurements

Mice were briefly anesthetized with isoflurane before cervical dislocation and decapitation. The brain was removed, sliced coronally on a 1-mm mouse brain matrix, a small tissue punch containing dorsal striatum was removed, flash frozen on dry ice and stored at −80 °C until all samples were collected. Glutamate, biogenic amines and major metabolites were measured by mass spectrometry by the Vanderbilt University Neurochemistry Core.

For neurotransmitter measurements experimental groups were as follows: WT veh = 3F, 2M; WT Mn = 5F, 4M; YAC128 veh =4F, 3M; YAC128 Mn = 4F, 5M.

2.9 Statistics

Data are reported as mean ± S.E.M. unless otherwise noted. Data analyses were completed in SPSS 26.0 or GraphPad Prism 8. In dietary intervention mice, we anticipated sex differences based on known sex differences observed in dietary Mn metabolism (Felber, Wu, & Zhao, 2019; Finley, Johnson, & Johnson, 1994) thus females and males were analyzed separately for all behavioral tests and molecular outcomes. Neurotransmitter and metabolite

concentrations from mice treated with Mn by subcutaneous injection (*see* Fig. 6) were first run with sex as a fixed variable. There were no differences according to sex, and thus all data were collapsed and analyzed together. FSCV data were not sufficiently powered to include sex as a variable (n=3-4 total mice per group). For all dependent variables, unless otherwise noted, two-way univariate ANOVA (2 genotype x 2 treatments) was conducted with appropriate post-hoc follow up tests. Outliers were removed only if they reflected experimental software error (e.g., beam tracking error in activity chambers) or if outside of 95% confidence interval ($\pm$ 2 standard deviations). The threshold for statistical significance for all tests was P < 0.05.

3. Results

3.1 Body weight and anxiety-like behavior were unaffected by high Mn diet in young mice

Mice were placed on experimental diets upon weaning (Fig. 1A). Mice on high Mn diet were similar weight compared to mice on control diet, suggesting that there were no overtly aversive reactions to the diet nor a propensity to eat more or less of the assigned diet. An anticipated genotype difference, in which YAC128 mice weighed more than WT, was confirmed in males (Genotype $F_{1, 28}$= 6.80, P=0.015, Diet $F_{1, 28}$=1.52, P=0.23) but was not significant in females (Genotype $F_{1, 21}$= 3.94, P=0.060, Diet $F_{1, 21}$=1.13, P=0.30; Fig. 1B). To ensure behavioral differences detected were not due to underlying anxiety-like phenotypes, mice were first tested on the elevated zero maze (EZM). In both males and females all genotype and diet groups spent a comparable proportion of time in the open zone confirming similar anxiety-like behavior in a novel testing environment (all Ps > 0.05; Fig. 1C).

3.2 Mn increased locomotor activity in young WT female mice

Despite similar time spent in the open zone of the EZM, female WT mice on high Mn diet were hyperactive compared to control diet (P=0.005) indicated by 1.49-fold greater distance travelled (m) during this 5-min task (Genotype $F_{1, 21}$= 0.28, P=0.60, Diet $F_{1, 21}$= 1.13, P=0.30, Interaction $F_{1, 21}$=16.82, P<0.0001), but Mn did not alter exploratory patterns of YAC128 females (Fig. 1D). In young male mice, neither Mn diet nor genotype affected distance travelled in the EZM (all Ps > 0.05; Fig. 1D). The hyperactive phenotype in young WT females on high Mn diet (P=0.008; 1.48-fold compared to control) was replicated in a second independent measure of locomotor activity over 30-min in the activity chambers (Genotype $F_{1, 21}$= 0.63, P=0.44, Diet $F_{1, 21}$= 4.31, P=0.051, Interaction $F_{1, 21}$=5.71, P=0.026, Fig. 1E). No activity differences were observed between groups for male mice (all Ps > 0.05; Fig. 1E).

Motor coordination and motor learning were assessed on the accelerated rotarod. Motor learning was intact in all groups based on improvement across training days (female - training day $F_{2, 42}$= 25.03, P < 0.0001, male - training day $F_{2, 56}$= 27.24, P < 0.0001). At this age, YAC128 mice did not display a rotarod performance deficit nor did high Mn diet alter rotarod performance in either genotype (all Ps > 0.05; Fig. 1F). Grip strength was assessed as an important control measure for rotarod performance and was similar among all (P > 0.05, Fig. 1G).

3.3 Behavior in aged mice was unaffected by high Mn diet

Body weight was measured weekly to monitor the health of the animals while on experimental diet beginning at 12 months of age (Fig. 2A). Weight change from 12 to 14 months of age was similar among mice on the control and high Mn diet in both sexes (Ps > 0.05). In females only, YAC128 mice weighed more overall and also gained more weight than WT although this was regardless of diet (Genotype $F_{1, 28}$=7.67, P=0.009; Fig. 2B). Overnight food consumption was measured when mice were singly housed for a nest building task. There were no significant differences between Mn diet groups nor genotype in the amount (g) of food consumed (P > 0.05; *data not shown*). Therefore, the high Mn chow was not acutely toxic and within a diet group each genotype was exposed to approximately the same level of Mn.

The behavioral battery was performed prior to diet intervention and after 8 weeks on experimental diet. Behavior for all tasks is shown as a fold change (post-experimental diet values normalized to baseline at 11.5 months of age) to avoid the expected confound of age-related decline on several tasks. Percent time spent in the open zone of the EZM was comparable among all groups at baseline prior to the diet change (30-33% time spent in open zone, within expected range (Eltokhi, Kurpiers, & Pitzer, 2020)), confirming absence of an anxiety-like phenotype that could affect results from other behavioral assays (Ps > 0.05; *data not shown*). Upon repeat testing at 14 months of age most mice spent less time exploring the open zones of the maze although there was no effect of high Mn diet on the fold change in time spent in the open zone of the EZM in either sex (P > 0.05). The decrease in time spent in the open zone was greater in YAC128 compared to WT in females, potentially due to increased anxiety-like behavior, reluctance to explore the maze, or simply a confounding effect of decreased locomotion in YAC128 females only (Genotype $F_{1, 27}$=7.07, P=0.013; Fig. 2C).

Fold change in distance travelled in the EZM was unaffected by high Mn diet (P > 0.05), but YAC128 females exhibited decreased activity during this 5-min task compared to WT females (Genotype $F_{1, 27}$=13.79, P=.0001; Fig. 2D). Similarly, fold change in total distance travelled during 30 min in the locomotor activity chambers was not impacted by high Mn diet (P > 0.05) but activity declined in YAC128 females more than WT females (Genotype $F_{1, 27}$=8.98, P=0.006) (Fig. 2E) with no genotype- or diet-related activity changes observed in males during either task (Fig. 2D–E). Prior to placement on experimental diet, YAC128 mice exhibited significant rotarod performance deficits, as expected, but were able to learn the task appropriately based on improvement across training days (Female: Genotype $F_{1, 27}$= 22.33, P<0.0001, Training day $F_{1, 27}$= 22.03, P<0.0001; Male: Genotype $F_{1, 15}$= 7.72, P=0.013, Training day $F_{1, 15}$= 16.71, P<0.0001; *raw data not shown*). Fold change in rotarod performance was not affected by high Mn diet, and performance declined in YAC128 compared to WT in the female mice only (Genotype $F_{1, 27}$=6.26, P=0.019) (Fig. 2F). Fold change in grip strength was comparable among all groups (Ps > 0.05) (Fig. 2G).

Mn exposure has been linked to spatial memory deficits in rodents (Lu et al., 2014) and humans (Bauer et al., 2017). However, no age-, genotype-, nor diet-related changes were observed in the percent spontaneous alternations made in the Y-maze, a hippocampal-dependent measure of spatial working memory (all Ps > 0.05; not shown). Nest building

is also shown to be hippocampal-dependent and reflects the personified behavior of overall well-being and ability to take care of oneself as well as some degree of executive function (C. L. C. Neely, Pedemonte, Boggs, & Flinn, 2019). This task was similarly unaffected by genotype and diet and the quality of nests were consistent as mice aged (all Ps > 0.05; not shown).

3.4   In young mice high Mn diet significantly increased striatal Mn concentration in both sexes but decreased total brain weight in females only

High Mn diet introduced at weaning significantly increased Mn levels in the striatum of both female (Diet $F_{1, 27}$= 4.45, P=0.044, Genotype $F_{1, 27}$= 2.07, P=0.16) and male mice at 12 weeks of age (Diet $F_{1, 27}$= 4.75, P=0.031, Genotype $F_{1, 27}$= 0.84, P=0.37) of both genotypes (Fig. 3A). Brains from female mice on high Mn diet weighed 2-6% less than brains from control diet female mice (Genotype $F_{1, 21}$= 7.55, P=0.012) at this age but no differences were observed in male mice (P > 0.05) (Fig. 3B).

3.5   High Mn diet altered tyrosine hydroxylase (TH) expression in young female but not male mice

To further probe the molecular mechanisms underlying the changes in locomotor activity in young female mice we examined expression differences in dopaminergic pathway proteins in the striatum. TH protein expression was differentially dependent on both genotype and Mn diet in females (Interaction $F_{1, 22}$= 2.01, P=0.0078). TH expression was decreased in YAC128 high Mn diet females compared to the elevated levels observed in control diet YAC128 females (P=0.045). TH expression increased 1.45-fold in WT female mice on high Mn diet, but this effect was not significant (P = 0.20). In males, TH expression was lower in YAC128 control diet mice compared to WT control diet (P=0.023) but high Mn diet did not significantly affect TH in either genotype of young male mice (Interaction $F_{1, 25}$=5.14, P=0.032; Fig. 3C). Expression of phosphorylated TH (pTH Ser31), the active form of this enzyme (Dunkley, Bobrovskaya, Graham, Von Nagy-Felsobuki, & Dickson, 2004), followed the same pattern as in females total TH expression but did not reach statistical significance (Interaction $F_{1, 22}$= 3.85, P=0.063) and no significant changes were detected in males (Interaction $F_{1, 25}$= 2.59, P=0.12; Fig. 3D). When examining pTH/TH there were no effects of genotype or diet in females (all Ps > 0.05) but in males, YAC128 mice had decreased expression compared to WT littermates (Genotype $F_{1, 25}$= 5.24, P=0.031; Fig. 3Ei). Representative blots are shown in Fig. 3Eii.

ERK1/2 is responsible for phosphorylating TH ser31 (Dunkley et al., 2004) and thus we measured total expression of this protein as well as its phosphorylated (active) form. There were no differences in total ERK expression based on genotype or diet in either sex (all Ps > 0.05). In males, pERK expression was increased overall in high Mn diet mice. The pERK/ERK ratio was not different between genotype and diet groups in females (all Ps > 0.05). In males, overall high Mn diet increased pERK/ERK ratio and YAC128 mice had decreased pERK/ERK (Genotype $F_{1, 24}$= 5.05, P=0.034, Diet $F_{1, 24}$= 5.26, P=0.031) (Fig. 3F) however, within each genotype the diet effect was not statistically significant.

The expression pattern of the dopamine reuptake transporter (DAT) observed in females among genotype and diet groups mimicked the pattern of TH expression, but was not significant (Interaction $F_{1, 19}$= 3.85, P=0.065) and there were no differences in DAT expression between groups in males (Fig. 3G).

3.6 Striatal Mn concentration was significantly increased in aged females on high Mn diet

Aged females on high Mn diet exhibited a significant increase in striatal Mn levels (Diet $F_{1, 25}$= 5.79, P=0.024) but no significant changes were detected in males (Diet $F_{1, 16}$= 0.011, P=0.92; Fig. 4A). There were no significant genotype differences in either sex (P > 0.05).

3.7 Brain weight was differentially altered by high Mn diet in aged WT and YAC128 mice

Total brain weight was lower in aged YAC128 mice compared to WT in both females (Genotype $F_{1,26}$= 14.90, P=0.0007) and males (Genotype $F_{1,16}$= 27.43, P=0.0001). In females, brain weight was decreased in high Mn diet compared to control diet (Interaction $F_{1,26}$= 5.70, P=0.025) in YAC128 only (P=0.024) but high Mn diet decreased brain weight similarly between genotypes in males (Diet $F_{1,15}$= 6.44, P=0.023) (Fig. 4B).

3.8 Dopaminergic synthesis proteins and DAT expression were unaffected by high Mn diet

TH was decreased in YAC128 female mice compared to WT at 14.5 months (Genotype $F_{1,27}$= 5.11, P=0.032), but Mn diet did not affect TH expression at this age in either sex or genotype (P > 0.05; Fig. 4C). Expression of pTH (Fig. 4D) and the pTH/TH ratio (Fig. 4E) were not significantly different according to genotype or Mn diet in either sex (all Ps > 0.05). Representative blots are shown in Fig. 4Eii. In both sexes, there were no differences in upstream protein ERK in its total expression, phosphorylated expression, nor the pERK/ERK ratio between genotype and Mn diet groups (all Ps > 0.05) (Fig. 4F).

DAT expression was subtly but not significantly increased by high Mn diet in female mice (Diet $F_{1,23}$= 3.75, P=0.06) with no significant changes in male mice (P > 0.05; Fig. 4G). When males and females were combined for analysis, DAT expression was significantly increased by high Mn diet and expression was lower in YAC128 (Diet $F_{1,39}$= 7.38, P=0.009, Genotype $F_{1,39}$= 4.62, P=0.038). Striatal SLC30A10 expression did not differ between YAC128 and WT and was not affected by Mn diet in either sex (all Ps > 0.05; not shown).

3.9 Mn differentially affected dopamine release and clearance in WT and YAC128 mice

To further probe these changes in the dopaminergic system *ex vivo* FSCV was used to measure dopamine release and clearance in middle-aged WT and YAC128 mice acutely exposed (3 injections over 1 week) to 50 mg/kg $MnCl_2 • 4(H_2O)$ (Fig. 5A) compared to vehicle. This dose is known to significantly increase striatal Mn concentrations (Dodd et al., 2005; Pfalzer et al., 2020). Mn did not change dopamine release, measured by peak current (nA), in Mn-exposed WT mice (Sidak's post-hoc P=0.81) but significantly increased dopamine release in YAC128 mice (post-hoc Sidak's P<0.0001) (Genotype $F_{1,86}$=27.09, P<0.0001, Treatment $F_{1,86}$=18.56 P<0.0001, Interaction $F_{1,86}$=12.07, P<0.0001; Fig. 5B). Mn exposure caused more rapid clearance of extracellular dopamine in WT mice, indicated by a shorter decay time (Tau, s), and dopamine was cleared more rapidly in YAC128

mice compared to WT regardless of treatment (Genotype $F_{1,84}$=48.54, P<0.0001, Interaction $F_{1,84}$=30.23, P<0.0001, post-hoc Sidak's P<0.0001; Fig. 5C). In WT mice Mn exposure effectively decreased the duration of dopamine in the synapse because dopamine release was not altered but clearance was increased. In contrast, in the YAC128 mice, faster dopamine clearance due to genotype was possibly corrected by increased dopamine release following Mn exposure which could potentially stabilize the availability of dopamine in the synapse.

3.10 Striatal dopamine metabolism was differentially altered by Mn in WT and YAC128 mice

Dopamine and its three major metabolites, 3-methoxytyramine (3-MT), homovanillic acid (HVA), and 3,4-dihydroxyphenylacetic acid (DOPAC) were measured from dorsal striatal tissue from WT and YAC128 mice acutely (1-week) exposed to Mn or vehicle (Fig. 6A). Dopamine tissue concentrations were significantly decreased by Mn (Genotype $F_{1,26}$=0.54, P=0.47, Treatment $F_{1,26}$=4.79, P=0.040, Interaction $F_{1,26}$=3.31, P=0.088; Fig. 6Bi). The main effect of treatment on dopamine concentration appears to be driven by the response observed in WT animals but the interaction did not reach statistical significance. Tissue concentrations of 3-MT were significantly decreased in WT Mn-exposed mice compared to vehicle (P=0.0044) but not in YAC128 mice (Genotype $F_{1,26}$=2.53, P=0.12, Treatment $F_{1,26}$=5.15, P=0.032, Interaction $F_{1,26}$=7.65, P=0.01; Fig. 6Bii). HVA was increased in YAC128 mice with no effect of Mn exposure in either genotype (Genotype $F_{1,27}$=5.56, P=0.030; Fig. 6Biii). DOPAC concentration was not significantly affected by either genotype or Mn exposure (all Ps > 0.05, Fig. 6Biv).

3.11 Mn decreased 5-HT and 5-HIAA but did not change norepinephrine (NE) concentration in striatum

Mn exposure decreased striatal tissue concentration of 5-HT regardless of genotype (Treatment $F_{1,28}$=6.101, P=0.012; Fig. 6Ci). Major metabolite 5-HIAA was increased overall in YAC128 compared to WT, but Mn exposure decreased 5-HIAA concentrations in both genotypes (Genotype $F_{1,28}$=7.004, P=0.013, Treatment $F_{1,28}$=6.74, P=0.015; Fig. 6Cii). There were no significant differences in norepinephrine (NE) concentration (all Ps > 0.05; Fig. 6D).

3.12 Decreased striatal glutamate concentration was corrected in Mn-exposed YAC128 mice

Tissue glutamate concentration was significantly lower in YAC128 vehicle mice compared to WT vehicle (P=0.025). Glutamate was increased in Mn-exposed YAC128 mice compared to YAC128 vehicle (P=0.032) and not significantly different from WT vehicle (P > 0.05) (Interaction $F_{1,31}$=07.45, P=0.0102; Fig. 6E).

4. Discussion

The present study demonstrated that age, sex, and the HD-genotype collectively affect Mn homeostasis; each of these variables influenced changes in behavior and the dopaminergic system as a result of excessive dietary Mn intake or acute systemic exposure. We hypothesized that in young mice, high Mn diet would cause adverse effects in WT and

prevent HD-phenotypes in YAC128. Our results examining locomotor behavior in young females support this hypothesized interaction. High Mn diet induced hyperactivity in two independent behavioral tasks in young WT females but not males. Regulation of locomotor activity is dependent on basal ganglia structures including striatum (Ortiz-Pulido et al., 2017) and dopamine is an important modulator of activity. Intranasal dopamine administration in C57Bl/6J is known to increase distance travelled in the open field and increase exploratory behavior in the elevated plus maze, with greater effects at lower dopamine doses (Kholodar, Amikishieva, & Anisimov, 2013). We identified increased TH, the rate-limiting enzyme in dopamine synthesis, in young female WT mice on high Mn diet though we did not observe increased pTH Ser 31, the active form of this enzyme, in these mice.

Although we report no changes in pTH or its upstream kinase ERK1/2, the hyperactive behavioral phenotype observed is consistent with behavioral outcomes in children exposed to Mn. Several studies have made associations between elevated peripheral Mn (blood and hair concentrations) and ADHD (Farias et al., 2010; Shih et al., 2018). However, null associations and even decreased hair Mn concentrations have also been reported in ADHD groups compared to neurotypical children (Soler-Blasco et al., 2020; Tinkov et al., 2020). Interestingly, when examining associations between Mn exposure and ADHD, effects are stronger in females than males, consistent with our results in the current study (Broberg et al., 2019; Farias et al., 2010). Increased prenatal exposure to Mn was also associated with poorer working memory and visuospatial ability in young girls and not boys, which highlights an age-specific window for increased sensitivity to detrimental effects from Mn exposure (Bauer et al., 2017).

We predicted high Mn diet in young YAC128 mice would prevent HD-behavioral phenotypes. Compared to WT, young female YAC128 mice on control diet travelled more in the EZM suggesting hyperactivity or increased exploratory behavior. Hyperactivity in YAC128 mice at 3 months of age has been previously reported (Slow et al., 2003). Additionally, risk-taking behavior is common in individuals with HD (McDonell et al., 2020) and although not significant, young female YAC128 mice in the current study spent more time in the open zone of the EZM in addition to the significant increase in distance travelled. Consistent with our behavioral findings and reports from others (Schwab et al., 2015), TH expression was increased in the striatum of these young YAC128 mice. Hyperactivity and elevated TH expression were normalized to WT levels by the high Mn diet, rescuing these HD-phenotypes. We sought to determine if high Mn diet could prevent motor coordination deficits in HD, but we did not detect an impairment in the control diet YAC128 mice at this age (11 weeks). We have previously reported significant motor coordination deficits in YAC128 mice at this age (Wilcox *et al., under review*) in the FVB/N background whereas the current study used C57B1/6J-YAC128 mice. Phenotypic severity is greater in YAC128 mice on the FVB/N background compared to C57B1/6J (Van Raamsdonk et al., 2007). No HD-behavioral phenotypes were present in young males, but TH expression was decreased in young YAC128 males on control diet compared to WT and the high Mn diet rescued this phenotype in males. TH expression in YAC128 mice was differentially altered between sexes, but high Mn diet corrected the phenotype in both sexes.

Females are more efficient at absorbing dietary Mn than males (Finley et al., 1994). Our behavioral findings in young mice further support this sex difference despite comparable increases in brain Mn between sexes. The mechanism responsible for the male-female difference in sensitivity to Mn toxicity is currently unknown. A recent study examining polymorphisms in the Mn transporters SLC30A10 and SLC39A8 suggests females are "genetically less efficient at regulating Mn" and polymorphisms in homeostatic proteins may underly this increased susceptibility to adverse outcomes following exposure (Broberg et al., 2019). Gut microbe differences between males and females may also explain these sex differences. In C57B1/6J mice, Mn exposure in drinking water (100 ppm for 13 weeks) was shown to differentially alter the gut microbiome and the gut-brain axis in a sex-specific manner with greater effects in females. A bi-directional relationship between Mn and gut microbiota was proposed such that Mn effects the microbiome composition, but the microbiota influence the sex sensitivity to Mn toxicity (Chi et al., 2017).

In aged mice, there were no significant sex differences in our behavioral measurements in relation to Mn diet or genotype. Further, we did not observe detrimental behavioral outcomes following high Mn diet in the aged mice despite a significant increase in striatal Mn in WT. Striatal Mn was not increased by high Mn diet in YAC128 mice. We have previously reported a Mn accumulation defect in HD cells and in YAC128 mice after acute subcutaneous injection (Pfalzer et al., 2020; Williams, Kwakye, et al., 2010; Williams, Li, et al., 2010), but this is the first report of a striatal Mn uptake deficit in YAC128 mice fed a high Mn diet.

We also illustrate that in striatal tissue following acute systemic Mn exposure the dopaminergic and glutamatergic neurotransmitter systems are differentially affected in WT and YAC128 mice of middle-age. Sex differences were not assessed in middle-aged mice because Mn was administered by systemic injection, bypassing the organ systems that may contribute in part to the sex-specific differences observed following dietary Mn exposure. YAC128 vehicle mice in the current study exhibited increased dopamine clearance from the synapse but similar dopamine release compared to WT vehicle, effectively decreasing the available dopamine in the synapse. Total dopamine tissue concentration was not significantly altered but major metabolite HVA was significantly increased in YAC128 mice regardless of Mn treatment suggesting increased dopaminergic activity. In a group of HD patients, plasma HVA levels were not altered in pre-symptomatic individuals with the genetic mutation for HD, but were significantly elevated in symptomatic individuals and were correlated with disease severity (Markianos, Panas, Kalfakis, & Vassilopoulos, 2009). Plasma HVA levels differed dependent on disease stage. In fact, many of the perturbations in the dopaminergic system in HD exhibit a biphasic pattern of dysfunction (Koch & Raymond, 2019). In pre-symptomatic and early-stage HD, dopamine levels are increased and contribute to presence of characteristic choreatic movements. Tyrosine hydroxylase (TH) levels and enzymatic activity are increased in early HD and perhaps as a compensatory mechanism, D1 and D2 receptors are reduced in early HD. In late-stage HD, the opposite trends are observed such that dopamine levels are decreased, TH levels and activity are reduced, but D1 and D2 receptor levels remain decreased (Koch & Raymond, 2019). Our YAC128 FSCV experimental results are consistent with symptomatic HD, given the decreased availability of dopamine in the synapse despite no changes in total dopamine concentration. This is to be

expected based on the age of these animals (8-9 months) (Van Raamsdonk et al., 2007). Mn treatment increased dopamine release in YAC128 mice, potentially stabilizing the available dopamine in the synapse given that clearance was unaffected in YAC128 mice. However, Mn treatment did not change concentration of dopamine or its metabolites in YAC128 mice.

In WT, Mn decreased the availability of dopamine in the synapse by increasing dopamine clearance but not affecting dopamine release. Total dopamine concentration and metabolite 3-MT were significantly lower in WT Mn-exposed mice than in WT vehicle. Reports on Mn-induced dopamine changes are inconclusive. A microdialysis study in rats found decreased dopamine release in the striatum after intrastriatal administration of $MnCl_2$ (Vidal et al., 2005). This reported functional outcome (decreased dopamine in the synapse) is consistent with more rapid clearance detected in our Mn-treated WT mice. Another study employing the same acute Mn exposure paradigm used here observed no effect of Mn on dopamine clearance but instead found that Mn decreased dopamine release (Khalid, Aoun, & Mathews, 2011). Dopamine can also be directly oxidized by Mn (Florence & Stauber, 1989). However, Mn can also increase spontaneous firing of dopamine neurons (Lin et al., 2019) and increase the binding of striatal vesicular monoamine transporter 2 (VMAT2) (Nguyen et al., 2003) thus potentially increasing dopamine in the synapse. Importantly, Mn altered dopamine clearance and tissue dopamine concentration and 3-MT concentration in WT but not YAC128 mice.

Glutamate concentration was differentially altered by Mn between YAC128 and WT mice. In WT mice, striatal glutamate was lower in Mn-exposed mice, but the effect was not significant. While not significant, these findings are consistent with decreased striatal glutamate following sub-chronic Mn exposure in rats (Nielsen, Larsen, Ladefoged, & Lam, 2017). It has been proposed that at higher Mn doses glutamate concentrations are increased (Erikson & Aschner, 2003). This may be related to decreased expression of glutamate transporters GLT-1 and GLAST (Lee, Karki, Johnson, Hong, & Aschner, 2017). In YAC128 mice, glutamate concentration was lower in vehicle treated mice compared to WT vehicle. Biphasic changes in glutamate have been reported in HD, similar to dopamine, such that increased glutamate is observed in early-stage and decreased glutamate is characteristic of late-stage HD. In YAC128 mice, Mn treatment increased glutamate concentration to a level that was not significantly different from WT vehicle.

Future studies are needed investigating the HD-Mn interaction at earlier developmental timepoints. The current study contributes to the growing body of research examining Mn homeostasis across age, sex, and disease states. Consistent with our original hypothesis, HD phenotypes were not ameliorated in aged YAC128 mice fed a high Mn diet. The corrective effect observed in young YAC128 females on high Mn diet suggests early intervention would be crucial and is influenced by sex. Our results show Mn affected the DA, 5-HT and glutamate neurotransmitter systems. Mn altered 5-HT and its metabolite 5-HIAA similarly in both WT and YAC128 mice. However, dopaminergic and glutamatergic systems were differentially altered by Mn in YAC128 and WT mice. Aberrant dopaminergic dynamics were potentially corrected in YAC128 by Mn exposure but YAC128 mice did not exhibit the decreases in dopamine and its metabolites that occurred in WT. Taken together, these findings suggest the differential status of the dopamine and glutamate systems in YAC128

may contribute to the decreased sensitivity to Mn toxicity and that any therapeutic effects of Mn in HD may act on these systems.

Acknowledgements:

References

André VM, Cepeda C, & Levine MS (2010). Dopamine and glutamate in huntington's disease: A balancing act. CNS Neuroscience and Therapeutics, 16(3), 163–178. 10.1111/j.1755-5949.2010.00134.x [PubMed: 20406248]

Balachandran RC, Mukhopadhyay S, McBride D, Veevers J, Harrison FE, Aschner M, … Bowman AB (2020). Brain manganese and the balance between essential roles and neurotoxicity. Journal of Biological Chemistry, 295(19), 6312–6329. 10.1074/jbc.REV119.009453

Bauer JA, Claus Henn B, Austin C, Zoni S, Fedrighi C, Cagna G, … Arora M (2017). Manganese in teeth and neurobehavior: Sex-specific windows of susceptibility. Environment International, 108, 299–308. 10.1016/j.envint.2017.08.013 [PubMed: 28941415]

Broberg K, Taj T, Guazzetti S, Peli M, Cagna G, Pineda D, … Wahlberg K (2019). Manganese transporter genetics and sex modify the association between environmental manganese exposure and neurobehavioral outcomes in children. Environment International, 130(March), 104908. 10.1016/j.envint.2019.104908 [PubMed: 31233999]

Chen P, Bornhorst J, & Aschner M (2018). Manganese metabolism in humans. Frontiers in Bioscience, 23, 1655–1679. 10.2741/4665

Chi L, Gao B, Bian X, Tu P, Ru H, & Lu K (2017). Manganese-induced sex-specific gut microbiome perturbations in C57BL/6 mice. Toxicology and Applied Pharmacology, 331, 142–153. 10.1016/j.taap.2017.06.008 [PubMed: 28610994]

Consoli DC, Brady LJ, Bowman AB, Calipari ES, & Harrison FE (2020). Ascorbate deficiency decreases dopamine release in gulo–/– and APP/PSEN1 mice. Journal of Neurochemistry, (June), 1–10. 10.1111/jnc.15151

Deacon RMJ (2006). Assessing nest building in mice. Nature Protocols, 1(3), 1117–1119. 10.1038/nprot.2006.170 [PubMed: 17406392]

Dodd CA, Ward DL, & Klein BG (2005). Basal ganglia accumulation and motor assessment following manganese chloride exposure in the C57BL/6 mouse. International Journal of Toxicology, 24(6), 389–397. 10.1080/10915810500366500 [PubMed: 16393931]

Dunkley PR, Bobrovskaya L, Graham ME, Von Nagy-Felsobuki EI, & Dickson PW (2004). Tyrosine hydroxylase phosphorylation: Regulation and consequences. Journal of Neurochemistry, 91(5), 1025–1043. 10.1111/j.1471-4159.2004.02797.x [PubMed: 15569247]

Eltokhi A, Kurpiers B, & Pitzer C (2020). Behavioral tests assessing neuropsychiatric phenotypes in adolescent mice reveal strain- and sex-specific effects. Scientific Reports, 10(1), 1–15. 10.1038/s41598-020-67758-0 [PubMed: 31913322]

Erikson KM, & Aschner M (2003). Manganese neurotoxicity and glutamate-GABA interaction. Neurochemistry International, 43(4–5), 475–480. 10.1016/S0197-0186(03)00037-8 [PubMed: 12742094]

Erikson KM, Thompson K, Aschner J, & Aschner M (2007). Manganese neurotoxicity: A focus on the neonate. Pharmacology and Therapeutics. 10.1016/j.pharmthera.2006.09.002

Farias AC, Cunha A, Benko CR, McCracken JT, Costa MT, Farias LG, & Cordeiro ML (2010). Manganese in children with attention-deficit/hyperactivity disorder Relationship with

methylphenidate exposure. Journal of Child and Adolescent Psychopharmacology, 20(2), 113–118. 10.1089/cap.2009.0073 [PubMed: 20415606]

Felber DM, Wu Y, & Zhao N (2019). Regulation of the metal transporters zip14 and znt10 by manganese intake in mice. Nutrients, 11(9). 10.3390/nu11092099

Fernandes J, Hao L, Bijli KM, Chandler JD, Orr M, Hu X, … Go Y-M (2017). Manganese Stimulates Mitochondrial H2O2 Production in SH-SY5Y Human Neuroblastoma Cells Over Physiologic as well as Toxicologic Range. Toxicol Sci, 155(1), 213–223. 10.1093/toxsci/kfw196 [PubMed: 27701121]

Finley JW, Johnson PE, & Johnson LK (1994). Sex affects manganese absorption and retention by humans from a diet adequate in manganese. The American Journal of Clinical Nutrition, 60(6), 949–955. 10.1093/ajcn/60.6.949 [PubMed: 7985639]

Fitsanakis VA, Au C, Erikson KM, & Aschner M (2006). The effects of manganese on glutamate, dopamine and γ-aminobutyric acid regulation. Neurochemistry International, 48(6–7), 426–433. 10.1016/j.neuint.2005.10.012 [PubMed: 16513220]

Florence TM, & Stauber JL (1989). Manganese catalysis of dopamine oxidation. Sci Total Environ, 78, 233–240. 10.1016/0048-9697(89)90036-3 [PubMed: 2541499]

Frisbie SH, Mitchell EJ, Roudeau S, Domart F, Carmona A, & Ortega R (2019). Manganese levels in infant formula and young child nutritional beverages in the United States and France: Comparison to breast milk and regulations. PloS One, 14(11), e0223636 10.1371/journal.pone.0223636 [PubMed: 31689314]

Frisbie SH, Ortega R, Maynard DM, & Sarkar B (2002). The concentrations of arsenic and other toxic elements in Bangladesh's drinking water. Environmental Health Perspectives, 110(11), 1147–1153. 10.1289/ehp.021101147 [PubMed: 12417487]

Gibson RS, Anderson BM, & Sabry JH (1983). The trace metal status of a group of post-menopausal vegetarians. Journal of the American Dietetic Association, 82(3), 246–250. [PubMed: 6298299]

Horning KJ, Caito SW, Tipps KG, Bowman AB, & Aschner M (2015). Manganese Is Essential for Neuronal Health. Annual Review of Nutrition, 35(1), 71–108. 10.1146/annurev-nutr-071714-034419

Jenkitkasemwong S, Akinyode A, Paulus E, Weiskirchen R, Hojyo S, Fukada T, … Knutson MD (2018). SLC39A14 deficiency alters manganese homeostasis and excretion resulting in brain manganese accumulation and motor deficits in mice. Proceedings of the National Academy of Sciences, 115(20), E4730. 10.1073/pnas.1806613115

Joshi PR, Wu NP, André VM, Cummings DM, Cepeda C, Joyce JA, … Bamford NS (2009). Age-dependent alterations of corticostriatal activity in the YAC128 mouse model of huntington disease. Journal of Neuroscience, 29(8), 2414–2427. 10.1523/JNEUROSCI.5687-08.2009 [PubMed: 19244517]

Kern CH, Stanwood GD, & Smith DR (2010). Preweaning manganese exposure causes hyperactivity, disinhibition, and spatial learning and memory deficits associated with altered dopamine receptor and transporter levels. Synapse (New York, N.Y.), 64(5), 363–378. 10.1002/syn.20736

Kern C, Stanwood G, & Smith DR (2011). Pre-weaning manganese exposure causes hyperactivity, disinhibition, and spatial learning and memory deficits associated with altered dopamine receptor and transporter levels. Control, 64(5), 363–378. 10.1002/syn.20736.Pre-weaning

Khalid M, Aoun RA, & Mathews TA (2011). Altered striatal dopamine release following a sub-acute exposure to manganese. Journal of Neuroscience Methods, 202(2), 182–191. 10.1016/j.jneumeth.2011.06.019 [PubMed: 21740928]

Kholodar AV, Amikishieva AV, & Anisimov MP (2013). Effects of intranasal administration of dopamine on anxiety and locomotor activity in two mouse strains. Neuroscience and Behavioral Physiology, 43(3), 409–415. 10.1007/s11055-013-9747-7

Kirkley KS, Popichak KA, Afzali MF, Legare ME, & Tjalkens RB (2017). Microglia amplify inflammatory activation of astrocytes in manganese neurotoxicity. Journal of Neuroinflammation, 14(1), 99. 10.1186/s12974-017-0871-0 [PubMed: 28476157]

Kitazawa M, Wagner JR, Kirby ML, Anantharam V, & Kanthasamy AG (2002). Oxidative stress and mitochondrial-mediated apoptosis in dopaminergic cells exposed to methylcyclopentadienyl

manganese tricarbonyl. The Journal of Pharmacology and Experimental Therapeutics, 302(1), 26–35. 10.1124/jpet.302.1.26 [PubMed: 12065696]

Koch ET, & Raymond LA (2019). Dysfunctional striatal dopamine signaling in Huntington's disease. Journal of Neuroscience Research, 97(12), 1636–1654. 10.1002/jnr.24495 [PubMed: 31304622]

Lasley SM, Fornal CA, Mandal S, Strupp BJ, Beaudin SA, & Smith DR (2020). Early Postnatal Manganese Exposure Reduces Rat Cortical and Striatal Biogenic Amine Activity in Adulthood. Toxicological Sciences, 173(1), 144–155. 10.1093/toxsci/kfz208 [PubMed: 31560393]

Lee E, Karki P, Johnson JJ, Hong P, & Aschner M (2017). Manganese Control of Glutamate Transporters' Gene Expression. Advances in Neurobiology, 16, 1–12. 10.1007/978-3-319-55769-4_1 [PubMed: 28828603]

Lin M, Colon-Perez LM, Sambo DO, Miller DR, Lebowitz JJ, Jimenez-Rondan F,… Khoshbouei H (2019). Mechanism of manganese dysregulation of dopamine neuronal activity. Journal of Neuroscience, 40(30), 5871–5891. 10.1101/792143

Lu CL, Tang S, Meng ZJ, He YY, Song LY, Liu YP, … Guo SC (2014). Taurine improves the spatial learning and memory ability impaired by sub-chronic manganese exposure. Journal of Biomedical Science, 21(1), 1–8. 10.1186/1423-0127-21-51 [PubMed: 24397824]

Madison JL, Wegrzynowicz M, Aschner M, & Bowman AB (2011). Gender and manganese exposure interactions on mouse striatal neuron morphology. Neurotoxicology, 32(6), 896–906. 10.1016/j.neuro.2011.05.007 [PubMed: 21641932]

Markianos M, Panas M, Kalfakis N, & Vassilopoulos D (2009). Plasma homovanillic acid and prolactin in huntington's disease. Neurochemical Research, 34(5), 917–922. 10.1007/s11064-008-9851-1 [PubMed: 18841471]

Martinez-Finley EJ, Gavin CE, Aschner M, & Gunter TE (2013). Manganese neurotoxicity and the role of reactive oxygen species. Free Radical Biology and Medicine, 62, 65–75. 10.1016/j.freeradbiomed.2013.01.032 [PubMed: 23395780]

Martins AC, Krum BN, Queirós L, Tinkov AA, Skalny AV, Bowman AB, & Aschner M (2020). Manganese in the Diet: Bioaccessibility, Adequate Intake, and Neurotoxicological Effects. Journal of Agricultural and Food Chemistry, 68(46), 12893–12903. 10.1021/acs.jafc.0c00641 [PubMed: 32298096]

McDonell KE, Ciriegio AE, Pfalzer AC, Hale L, Shiino S, Riordan H, … Claassen DO (2020). Risk-Taking Behaviors in Huntington's Disease. Journal of Huntington's Disease, 9(4), 359–369. 10.3233/JHD-200431

Neely CLC, Pedemonte KA, Boggs KN, & Flinn JM (2019). Nest building behavior as an early indicator of behavioral deficits in mice. Journal of Visualized Experiments, 2019(152), 1–8. 10.3791/60139

Neely MD, Davison CA, Aschner M, & Bowman AB (2017). Manganese and Rotenone-Induced Oxidative Stress Signatures Differ in iPSC-Derived Human Dopamine Neurons. Toxicol Sci, 159(2), 366–379. 10.1093/toxsci/kfx145 [PubMed: 28962525]

Nguyen HOX, Goracke-Postle CJ, Kaminski LL, Overland AC, Morgan AD, & Fairbanks CA (2003). Neuropharmacokinetic and Dynamic Studies of Agmatine (Decarboxylated Arginine). Annals of the New York Academy of Sciences, 1009, 82–105. 10.1196/annals.1304.009 [PubMed: 15028573]

Nielsen BS, Larsen EH, Ladefoged O, & Lam HR (2017). Subchronic, Low-Level Intraperitoneal Injections of Manganese (IV) Oxide and Manganese (II) Chloride Affect Rat Brain Neurochemistry. International Journal of Toxicology, 36(3), 239–251. 10.1177/1091581817704378 [PubMed: 28460583]

Ortiz-Pulido R, Hernández-Briones ZS, Tamariz-Rodríguez A, Hernández ME, Aranda-Abreu GE, Coria-Avila GA, … García LI (2017). Effect of electrolytic lesion of the dorsomedial striatum on sexual behaviour and locomotor activity in rats. Neurología (English Edition), 32(5), 278–283. 10.1016/j.nrleng.2015.11.008

Pfalzer AC, Wilcox JM, Codreanu SG, Totten M, Bichell TJV, Halbesma T, … Bowman AB (2020). Huntington's disease genotype suppresses global manganese-responsive processes in pre-manifest and manifest YAC128 mice. Metallomics, 12(7), 1118–1130. 10.1039/d0mt00081g [PubMed: 32421118]

Robison G, Sullivan B, Cannon JR, & Pushkar Y (2015). Identification of dopaminergic neurons of the substantia nigra pars compacta as a target of manganese accumulation†‡. Metallomics, 7(5), 748–755. 10.1039/c5mt00023h [PubMed: 25695229]

Schuh MJ (2016). Possible Parkinson's Disease Induced by Chronic Manganese Supplement Ingestion. Consult Pharm, 31(12), 698–703. 10.4140/TCP.n.2016.698 [PubMed: 28074748]

Schullehner J, Thygesen M, Kristiansen SM, Hansen B, Pedersen CB, & Dalsgaard S (2020). Exposure to Manganese in Drinking Water during Childhood and Association with Attention-Deficit Hyperactivity Disorder: A Nationwide Cohort Study. Environmental Health Perspectives, 128(9), 97004. 10.1289/EHP6391 [PubMed: 32955354]

Schwab LC, Garas SN, Drouin-Ouellet J, Mason SL, Stott SR, & Barker RA (2015). Dopamine and Huntington's disease. Expert Review of Neurotherapeutics, 15(4), 445–458. 10.1586/14737175.2015.1025383 [PubMed: 25773746]

Shih J-H, Zeng B-Y, Lin P-Y, Chen T-Y, Chen Y-W, Wu C-K, … Wu M-K (2018). Association between peripheral manganese levels and attention-deficit/hyperactivity disorder: a preliminary meta-analysis. Neuropsychiatric Disease and Treatment, 14, 1831–1842. 10.2147/NDT.S165378 [PubMed: 30140155]

Slow EJ, van Raamsdonk J, Rogers D, Coleman SH, Graham RK, Deng Y, … Hayden MR (2003). Selective striatal neuronal loss in a YAC128 mouse model of Huntington disease. Human Molecular Genetics, 12(13), 1555–1567. 10.1093/hmg/ddg169 [PubMed: 12812983]

Soler-Blasco R, Murcia M, Lozano M, González-Safont L, Amorós R, Ibarluzea J, … Llop S (2020). Prenatal manganese exposure and neuropsychological development in early childhood in the INMA cohort. International Journal of Hygiene and Environmental Health, 224, 113443. 10.1016/j.ijheh.2019.113443 [PubMed: 31978738]

Taylor CA, Hutchens S, Liu C, Jursa T, Shawlot W, Aschner M, … Mukhopadhyay S (2019). SLC30A10 transporter in the digestive system regulates brain manganese under basal conditions while brain SLC30A10 protects against neurotoxicity. Journal of Biological Chemistry, 294(6), 1860–1876. 10.1074/jbc.RA118.005628

Tinkov AA, Mazaletskaya AL, Ajsuvakova OP, Bjørklund G, Huang PT, Chernova LN, … Skalny AV (2020). ICP-MS Assessment of Hair Essential Trace Elements and Minerals in Russian Preschool and Primary School Children with Attention-Deficit/Hyperactivity Disorder (ADHD). Biological Trace Element Research, 196(2), 400–409. 10.1007/s12011-019-01947-5 [PubMed: 31691190]

Tran TT, Chowanadisai W, Lönnerdal B, Le L, Parker M, Chicz-Demet A, & Crinella FM (2002). Effects of neonatal dietary manganese exposure on brain dopamine levels and neurocognitive functions. Neurotoxicology, 23(4–5), 645–651. 10.1016/s0161-813x(02)00068-2 [PubMed: 12428736]

Van Raamsdonk JM, Metzler M, Slow E, Pearson J, Schwab C, Carroll J, … Hayden MR (2007). Phenotypic abnormalities in the YAC128 mouse model of Huntington disease are penetrant on multiple genetic backgrounds and modulated by strain. Neurobiology of Disease, 26(1), 189–200. 10.1016/j.nbd.2006.12.010 [PubMed: 17276692]

Vidal L, Alfonso M, Campos F, Faro LRF, Cervantes RC, & Durán R (2005). Effects of manganese on extracellular levels of dopamine in rat striatum: An analysis in vivo by brain microdialysis. Neurochemical Research, 30(9), 1147–1154. 10.1007/s11064-005-7775-6 [PubMed: 16292508]

Wang D, Zhang J, Jiang W, Cao Z, Zhao F, Cai T, … Luo W (2017). The role of NLRP3-CASP1 in inflammasome-mediated neuroinflammation and autophagy dysfunction in manganese-induced, hippocampal-dependent impairment of learning and memory ability. Autophagy, 13(5), 914–927. 10.1080/15548627.2017.1293766 [PubMed: 28318352]

Warren EB, Bryan MR, Morcillo P, Hardeman KN, Aschner M, & Bowman AB (2020). Manganese-induced Mitochondrial Dysfunction Is Not Detectable at Exposures Below the Acute Cytotoxic Threshold in Neuronal Cell Types. Toxicol Sci, 176(2), 446–459. 10.1093/toxsci/kfaa079 [PubMed: 32492146]

Wilcox JM, Pfalzer AC, Tienda AA, Debbiche IF, Cox EC, Totten MS, … Bowman AB (2021). YAC128 mouse model of Huntington disease is protected against subtle chronic manganese (Mn)-induced behavioral and neuropathological changes. Nenrotoxicology, 87, 94–105. 10.1016/j.neuro.2021.09.002

Williams BB, Kwakye GF, Wegrzynowicz M, Li D, Aschner M, Erikson KM, & Bowman AB (2010). Altered manganese homeostasis and manganese toxicity in a huntington's disease striatal cell model are not explained by defects in the iron transport system. Toxicological Sciences, 10.1093/toxsci/kfq174

Williams BB, Li D, Wegrzynowicz M, Vadodaria BK, Anderson JG, Kwakye GF, … Bowman AB (2010). Disease-toxicant screen reveals a neuroprotective interaction between Huntington's disease and manganese exposure. Journal of Neurochemistry, 112(1), 227–237. 10.1111/j.1471-4159.2009.06445.X [PubMed: 19845833]

Winslow JWW, Limesand KH, & Zhao N (2020). The functions of ZIP8, ZIP14, and ZnT10 in the regulation of systemic manganese homeostasis. International Journal of Molecular Sciences, 21(9). 10.3390/ijms21093304

Yang Y, Ma S, Wei F, Liang G, Yang X, Huang Y, … Zou Y (2019). Pivotal role of cAMP-PKA-CREB signaling pathway in manganese-induced neurotoxicity in PC12 cells.. Environmental Toxicology, 34(9), 1052–1062. 10.1002/tox.22776 [PubMed: 31161640]

Yorgason JT, España RA, & Jones SR (2011). Demon voltammetry and analysis software: analysis of cocaine-induced alterations in dopamine signaling using multiple kinetic measures. Journal of Neuroscience Methods, 202(2), 158–164. 10.1016/j.jneumeth.2011.03.001 [PubMed: 21392532]
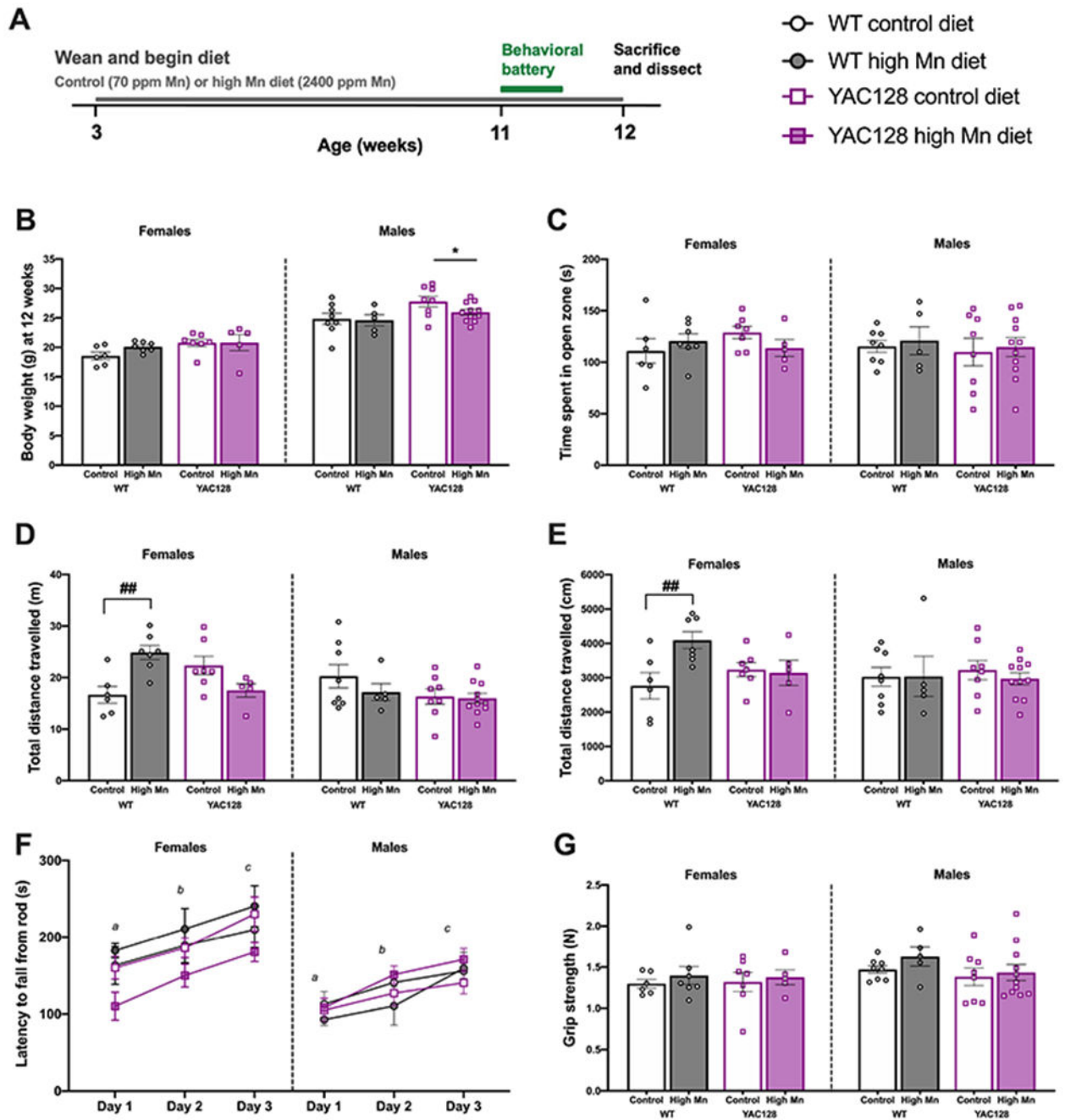
Figure 1. Behavioral data for young mice on experimental diet.
(**A**) Experimental timeline. (**B**) The diet did not alter weight gain in any group, but males weighed more than females and YAC128 mice weighed more than WT. (**C**) There was no anxiety phenotype detected in any group based on time spent in the open zone of the EZM. (**D**) In WT females, the high Mn diet induced hyperactivity measured by distance travelled during the EZM. (**E**) WT females on high Mn diet were hyperactive as measured by total distance travelled over 30 min in locomotor activity chambers (post-hoc Sidak's multiple comparisons). (**F**) There were no impairments in rotarod performance and motor learning

was intact indicated by significant improvement over training days. Days that do not share a superscript are significantly different from each other. **(G)** Grip strength was similar among all genotype and diet groups. For all, mean ± S.E.M. plotted unless otherwise noted. n=5-7 per genotype-diet group for females and n=5-11 for males. *P<0.05 indicates main effect of genotype. #P<0.05, ##P<0.01 indicates significant effect of Mn within genotype following a significant interaction (post-hoc Sidak's multiple comparisons).
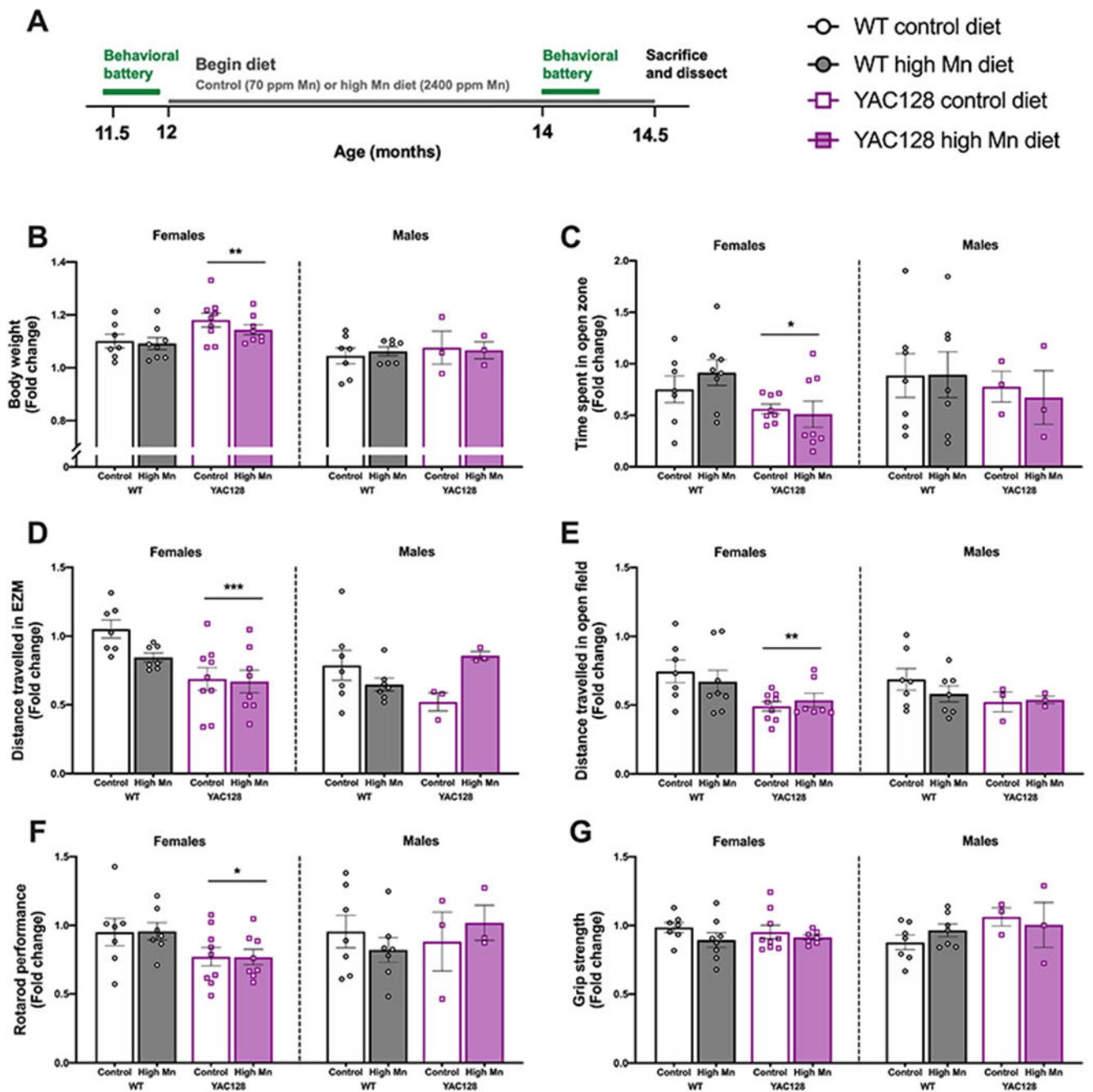
Figure 2. Behavioral data for aged mice on experimental diet.
(**A**) Experimental timeline. All behavior is plotted as fold change (post-experimental diet normalized to baseline performance at 12 months). (**B**) Change in body weight was not affected by diet. YAC128 mice were heavier and gained more weight over time in females only. (**C**) Fold change in the time spent in the open zone of the EZM. The decrease in time spent in the open zone was greater in female YAC128 mice compared to WT, with no effect of high Mn diet in any group. (**D**) Fold change in distance travelled during the EZM task was unaffected by high Mn diet in both sexes, but the change in distance travelled was greater

in YAC128 than WT in females only. **(E)** Fold change in the total distance travelled during 30 min in locomotor activity chambers. No effects of high Mn diet but again the decrease in activity was greater in YAC128 females than WT females. **(F)** Fold change in rotarod performance was significantly different between WT and YAC128 in females only, with no effect of high Mn diet in either sex. **(G)** Fold change in grip strength was comparable among all groups. For all, mean ± S.E.M. plotted unless otherwise noted. n=7-9 per genotype-diet group for females and n=3-7 for males. *P <0.05, *Pp<0.01, ***P<0.001 indicates main effect of genotype.
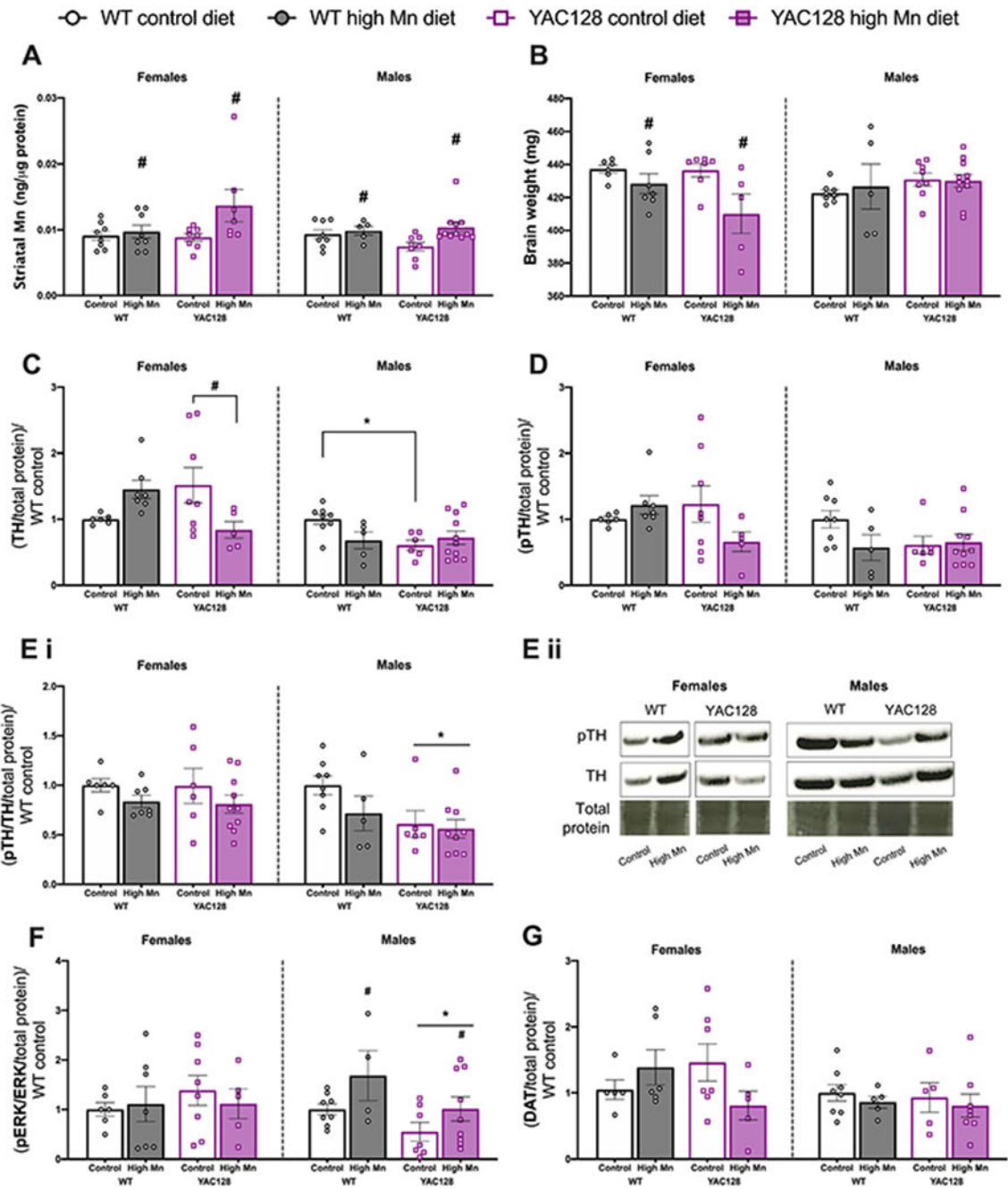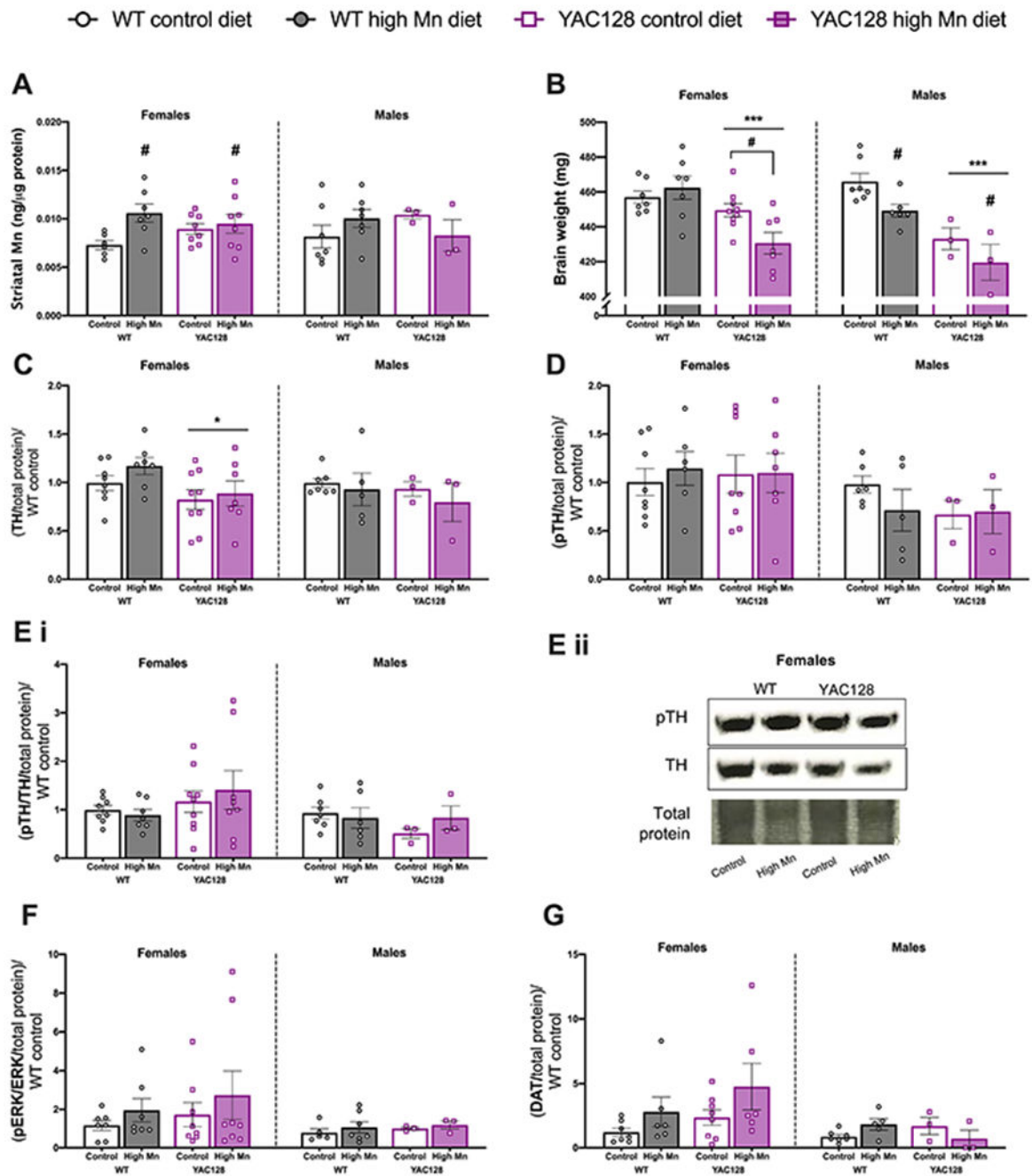
Figure 3.

*Diet induced brain changes in young mice. (**A**) Striatal Mn concentration was significantly increased in females and males on high Mn diet with no differences between genotypes. (**B**) Brain weight was significantly lower in females on high Mn diet compared to control diet with no effect of genotype. No differences in brain weight were observed in males. (**C**) Tyrosine hydroxylase (TH) was decreased in YAC128 females on high Mn diet compared to YAC128 control diet. TH expression was significantly lower in YAC128 control diet males compared to WT. (**D**) Phosphorylated TH (pTH Ser 31) expression followed a similar*

pattern as total TH but differences were not statistically significance. (***E***) *(i) No effect of genotype nor diet on pTH/TH ratio in females. YAC128 males had overall decreased pTH/TH ratio compared to WT regardless of diet. (ii) Representative blot images for changes pTH and TH in females (left) and males (right). For all western blots in young mice, sexes were run on separate blots and therefore should not be directly compared to each other.* (***F***) *No effect of genotype nor diet in females on pERK/ERK expression*, but in males, overall high Mn diet increased pERK/ERK ratio and YAC128 mice had decreased pERK/ERK. (***G***) *DAT expression was not significantly different among groups. For all, mean ± S.E.M. plotted unless otherwise noted. n= 5-8 per genotype-diet group for females and n=5-11 per group for males. *P<0.05 main effect of genotype, #P<0.05 main effect of Mn except where specific pairs are indicated with a horizontal bracket denoting Sidak's post-hoc comparisons following a significant interaction.*
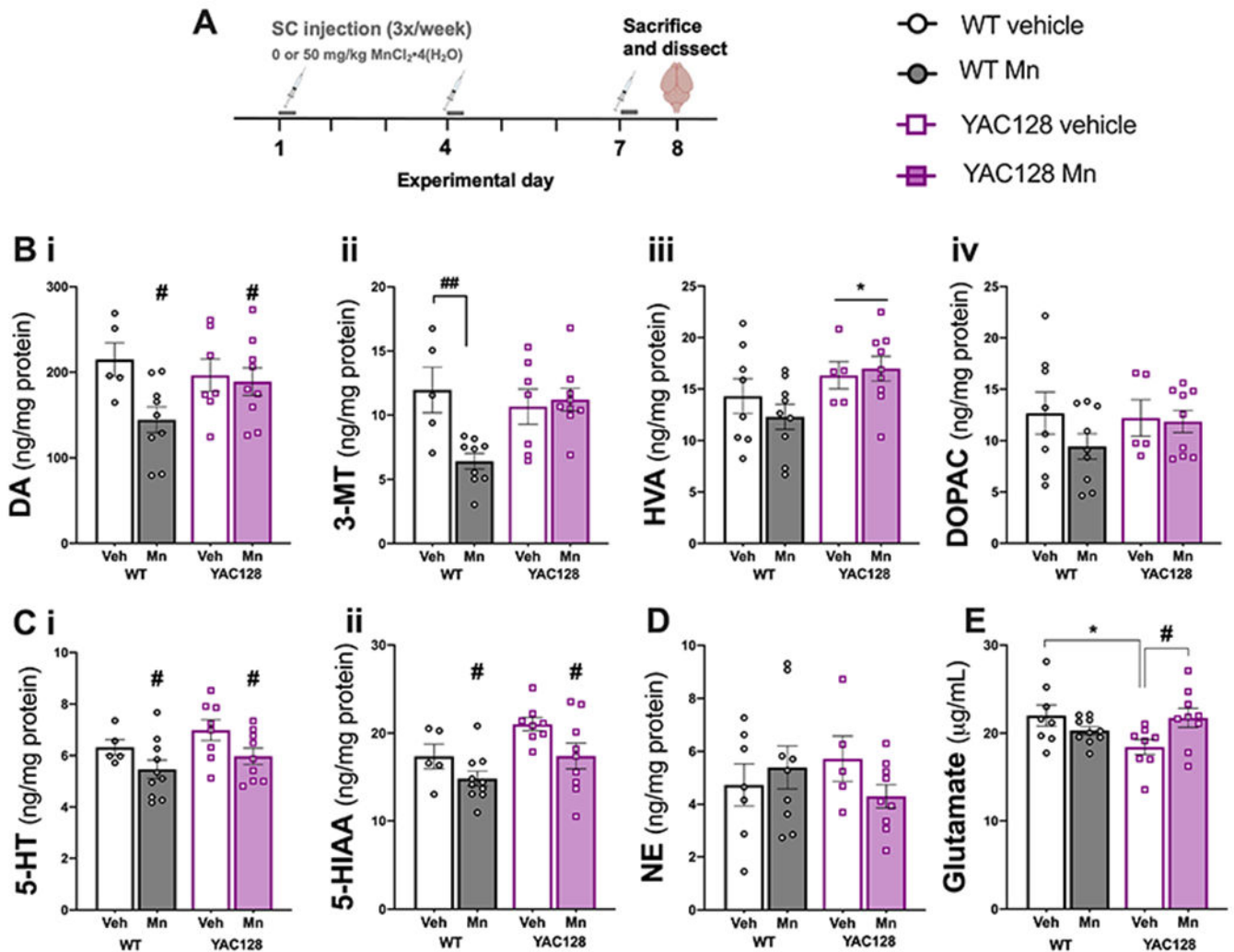
Figure 4.
Diet induced brain changes in aged mice. (**A**) Striatal Mn concentration was significantly increased by high Mn diet in females but not males. (**B**) Brain weight was significantly lower in YAC128 mice compared to WT in both sexes. Brains from female YAC128 mice on high Mn diet weighed significantly less than YAC128 mice on control diet. Brains from males on high Mn diet weighed less than those on control diet. (**C**) TH expression was lower in YAC128 females compared to WT females, with no effect of diet in either sex. (**D**) There were no differences in pTH Ser 31 nor (**E**i) the pTH/TH ratio among genotype and diet

groups in either sex. (**E**ii) Representative blots for pTH and TH in females only. **(F) No significant changes in pERK/ERK expression. (G)** DAT expression was not significantly increased in groups on high Mn diet. n=6-9 per genotype-diet group for females, n=3-7 per genotype-diet group for males. For all, mean ± S.E.M. plotted unless otherwise noted. *$P<0.05$, **$P<0.01$, ****$P<0.0001$ indicate main effect of genotype, # $P<0.05$ indicates a main effect of Mn effect except where specific pairs are indicated with a horizontal bracket denoting Sidak's post-hoc comparisons following a significant genotype x treatment interaction.
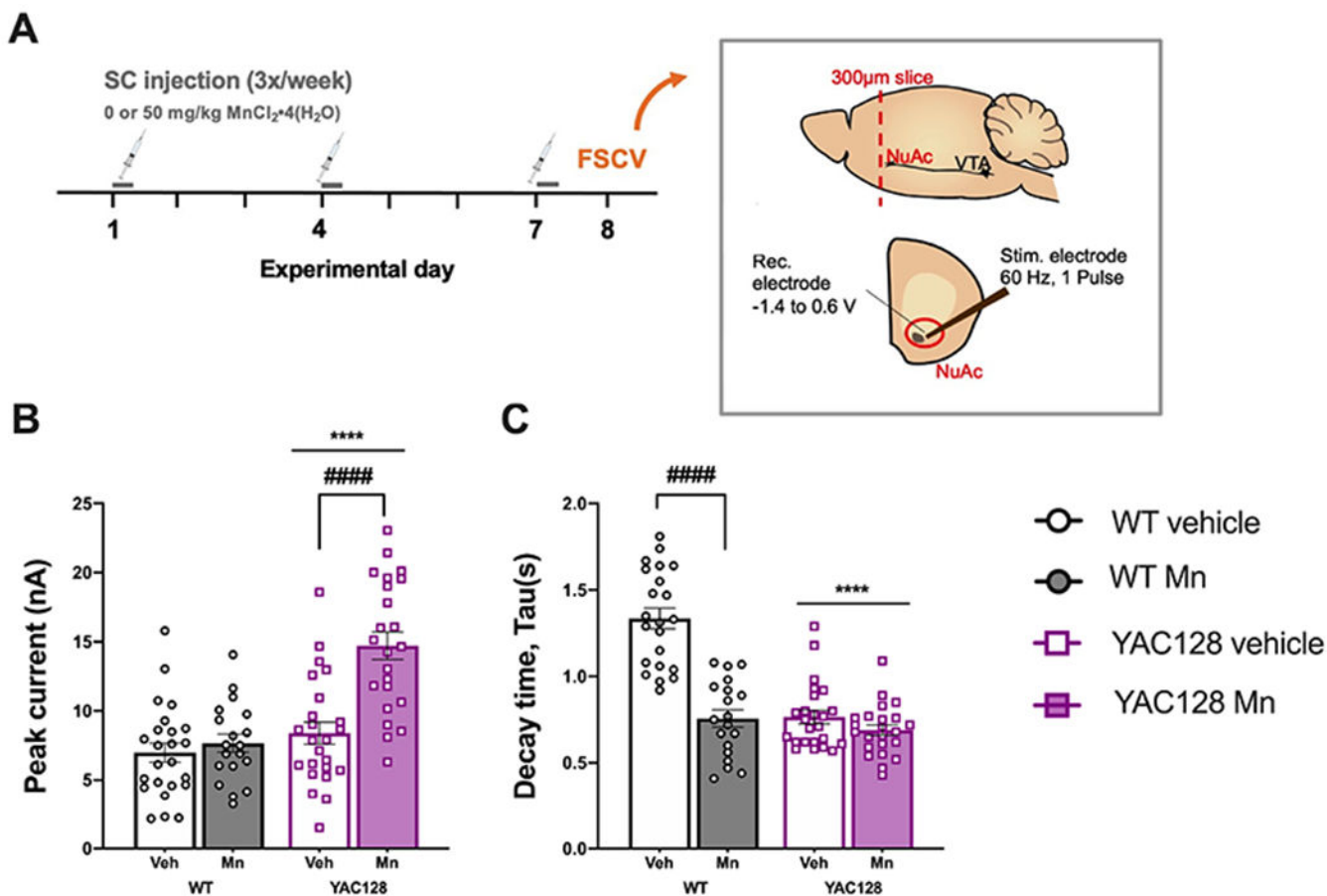
Figure 5. Dopamine release and clearance in middle-aged Mn-exposed mice.
(A) Experimental timeline. Inset image adapted from Consoli et al., 2020. NuAc, nucleus accumbens; VTA, ventral tegmental area. **(B)** Mn did not impact dopamine release in WT but significantly increased dopamine release in YAC128, **(C)** Dopamine clearance as indicated by decay time. Mn increased the rate of dopamine clearance (decreased tau) in WT mice. Clearance was significantly more rapid in YAC128 mice compared to WT with no effect of Mn. Mean ± S.E.M. plotted. n=3-5 mice per genotype-treatment group, approximately equal males and females per group, n=6-8 slices per mouse. ****P<0.0001 main effect of genotype, ####P<0.0001 significant effect of Mn within genotype Sidak's post-hoc comparisons following a significant genotype x treatment interaction in pairs of groups as marked with a horizontal bracket.

Figure 6. Neurotransmitter and metabolite measurements from dorsal striatum of middle-aged Mn-exposed mice.

(A) Experimental timeline. **(B)** Mn exposure decreased (i) dopamine (DA), (ii) Mn exposure decreased 3-MT in WT only, (iii) HVA was increased in YAC128 mice and (iv) there were no significant differences in DOPAC. **(C)** (i) 5-HT and its metabolite (ii) 5-HIAA were decreased in both genotypes by Mn exposure. **(D)** NE levels were not significantly different among groups. **(E)** Glutamate was significantly lower in YAC128 vehicle mice compared to WT vehicle. Mn exposure increased glutamate in YAC128 to levels not significantly different from WT vehicle. Data shown are mean ± S.E.M.. n=5-9 mice per group, approximately equal number males and females. *P<0.05 main effect of genotype, #, P<0.05, ##P<0.01 main effect of Mn treatment or differences between pairs of group data as marked with a horizontal bracket indicating significant Sidak's post-hoc following a significant genotype x treatment interaction.